Translational Oncology 15 (2022) 101261

Contents lists available at ScienceDirect

Translational Oncology

journal homepage: www.elsevier.com/locate/tranon

Original Research

Exposure to Tobacco Smoking Induces a subset of Activated Tumor-resident Tregs in Non-Small Cell Lung Cancer

Yudi Hu [a,b,c,1], Chaoqun Xu [a,b,c,1], Jun Ren [d], Yuanyuan Zeng [a,b,c], Fengyang Cao [a,b,c], Hongkun Fang [a,b,c], Guo Jintao [a,b,c], Ying Zhou [a,b,c,*], Qiyuan Li [a,b,c,*]

[a] National Institute for Data Science in Health and Medicine, Xiamen University, Xiamen, 361102, China
[b] Department of hematology, School of Medicine, Xiamen University, Xiamen, 361102, China
[c] Department of Pediatrics, The First Affiliated Hospital of Xiamen University, Xiamen, 361102, China
[d] School of Informatics, Xiamen University, Xiamen, 361105, China

ARTICLE INFO

Keywords:
Lung cancer
Single cell
Tumor immune microenvironment
Smoking
Treg

ABSTRACT

Tobacco smoking is the major cause of non-small-cell-lung cancer (NSCLC). However, it is barely known how smoking impact the tumor immune environment (TIME) of lung cancer.

We integrated single-cell RNA-seq and bulk RNA-seq data from several studies to systematically study the impact of smoking on T cells in treatment naïve NSCLC patients. We defined a set of smoking-induced differentially expressed genes (SIDEGs) in different cells in TIME.. Specifically, we defined a smoking-related tumor-specific Treg subset, ADAM12^{+} CTLA4^{+} Tregs according to the trajectory analysis and highly express genes in cell adhesion pathways and lipid metabolism. Using independent datasets from treatment naïve patients, we found that the fraction of ADAM12^{+} CTLA4^{+} Tregs are significantly increased in patients with smoking history. Moreover, the fraction of ADAM12^{+} CTLA4^{+} Tregs are positively correlated with the fraction of exhausted T cells. Additionally, we reconstructed the spatial organization of the tumor immune microenvironment and found that ADAM12^{+} CTLA4^{+} Tregs more actively communicate with LAYN^{+}CD8^{+} exhausted T cells compared with ADAM12^{-}CTLA4^{+} Tregs.

Our data demonstrate that smoking induced a unique subset of tumor-specific activated Tregs which interact with exhausted T cells in the TIME. Our findings not only explained how smoking impact the TIME but also provide new targets and biomarkers for precision immunotherapy of lung cancer.

Introduction

Non-small-cell lung cancer (NSCLC) accounts for ~85% of lung cancers and is the major cause of cancer-death [1]. Smoking is the top risk factor of NSCLC and contributes higher mortality [2]. It is reported that cigarette smoke exposure significantly increased the numbers of lung metastases following tumor challenge [3]. Moreover, *in utero* exposure to components of cigarette smoke increases the life-long risk of cancer in human, and this is replicated in mouse models [4]. The mechanism underlying smoking increasing the risk of cancer has been studied extensively. The main theory is that the carcinogens of cigarette smoke, such as benzo[*a*]pyrene (BP), causes extensive genomic alterations [5], in particular, a large number of C-to-A somatic mutations in human and forms "smoking mutational signature" [6]. In turn, the somatic mutations can result in loss-of-function mutation in tumor suppressor P53 [7] and gain-of-function in oncogene KRAS [8]. More importantly, high mutational burdens caused by smoking in tumor can yield large amount of neoantigens, and reshape the tumor immune microenvironment [9].Besides, a high mutational burden was related to better response to immune checkpoint blockade [10].

Cancer immunotherapies have shown sustained clinical responses in treating NSCLC, but efficacy varies. Studies shown that smoking status influence the response of PD-1 immunotherapies probably due to the somatic mutational burden elicited by smoking [6]. Epidemiologic studies also showed that NSCLC patients with smoking history experience a higher overall response rate (ORR) of immunotherapy than non-smokers [11,12]. However, the mechanism underlying the difference between smoker patients and non-smoker patients remains

* Corresponding authors: National Institute for Data Science in Health and Medicine, School of Medicine, Xiamen University, Xiamen, 361102, China.
E-mail addresses: yingzhou@xmu.edu.cn (Y. Zhou), qiyuan.li@xmu.edu.cn (Q. Li).
[1] These authors contributed equally to this work.

https://doi.org/10.1016/j.tranon.2021.101261
Received 17 August 2021; Received in revised form 26 October 2021; Accepted 28 October 2021

undetermined. We suspect that smoking status influences the composition and properties of tumor-infiltrating lymphocytes (TILs) since the amount and properties of TILs are known to affect the efficacy of immunotherapy [10,13,14]. However, how smoking status affects intra-tumoral heterogeneity, especially the composition of the tumor microenvironment of the lung cancer is largely unknown. It is critical to understand the dynamics and diversity of TILs influenced by smoking since the diversity of TILs contributes to diverse response to cancer immunotherapies. Among TILs, regulatory T cells (Tregs) are one of the most important T cell subsets in the tumor microenvironment. Tregs are a sub group of CD4 T cells and have a strong immunosuppressive function. Infiltration of Treg cells into the tumor immune microenvironment (TIME) occurs in multiple cancer types [15]. Tregs directly suppress anti-tumor immune response and promote the occurrence and development of tumors [16]. The role of Tregs in TME includes secreting inhibitory cytokines, killing effector cells by granulase and perforin, interfering with effector cells' metabolism and affecting DCs and macrophages [17]. Depletion of Tregs in tumors is arising as an attractive strategy for tumor immunotherapies [18]. In this study, we further characterized the subsets of Tregs in TIME and discovered potential targets for Tregs interference.

The conventional bulk RNA-seq technologies have been widely used to study gene expression patterns at population level to identify novel therapeutic targets and diagnostic markers of lung cancer in the past decade [19–21]. However, the traditional transcriptomic investigation is based on mixture cellular populations, which lacks sufficient resolution in the identification of specific cellular types and is unable to determine the intra-tumoral heterogeneity as well as the complexity and diversity of the TIME and its influence on response to therapies [22,23]. The advent of single-cell RNA sequencing (scRNA-seq) provides unprecedented opportunities for exploring gene expression profile at the single-cell level and has become a promising choice for exploring the key questions of intra-tumoral heterogeneity [24–26] and the cellular cross-talk within the TIME [27–29].

Several single-cell RNA sequencing (RNA-seq) studies have revealed diverse subsets and functions of T cells in various cancer types [22,25,30,31] including NSCLC [22,23]. Single-cell studies have shown that smoking can alter the cellular composition and epithelial function in tracheal epithelium [32] and bronchial epithelium [33], and peripheral blood [34]. However, so far, there are no single-cell studies focusing on smoking-induced aberrant TIME in lung cancer. Therefore, in this study, we determine to depict the impact of smoking on the landscape of the composition, spatial interactions and functions of TILs in NSCLC. Here we performed an integrated analysis of single-cell RNA seq [22,23] and bulk-RNA seq data [35] of total 109 treatment-naïve NSCLC patients with smoking history to decipher the impact of smoking induced aberrant microenvironment in primary tumor, distant metastases, adjacent normal tissues and peripheral blood from treatment-naïve NSCLC patients, including 106 adenocarcinomas and 3 squamous cell carcinomas.

Materials and methods

Data source

We downloaded processed single-cell transcriptome data (accession number: GSE99254, GSE131907 and GSE138867) from the Gene Expression Omnibus (GEO) database (https://www.ncbi.nlm.nih.gov/geo/). Bulk RNA-seq dataset of 51 NSCLC patients with 51 tumor tissues and matched 49 normal tissues are downloaded from Cell,2020 [35] (https://ars.els-cdn.com/content/image/1-s2.0-S0092867420306760-mmc3.xlsx). The summarized data information is in Supplementary Table 1 and Fig.1a. Clinical data are summarized in Supplementary Table 2 which include age, gender, smoking status, Tumor stage. We only include treatment naïve patients since the tumor immune microenvironments are known to change after targeted or immunotherapies. The RNA-seq datasets were classified into primary tumor, normal, blood, distant metastases groups (Supplementary Table 2). For GSE99254 dataset, we analyzed 9055 T cells of the 16 clusters from 14 patients, including 7 for conventional $CD4^+$ T cells, 7 for $CD8^+$ T cells, and 2 for regulatory T cells. For GSE131907 dataset, we selected T lymphocytes cells (203,298 cells) from the original study and annotated them according to GSE99254 and performed further analysis.

Single cell gene differential expression and gene ontology enrichment analysis

To investigate the impact of the smoking status on blood, normal lung and tumor tissue immune microenvironment, we performed a generalized linear regression using the T cell expression data from Guo et al. study to study the smoking-induced differentially expressed genes (SIDEGs) in blood, normal and tumor tissues in male and female, respectively. We first stratified the data by sex and tissue and we, then, used the "fitModel" function from Monocle 3 [36–38] to identify SIDEGs by performing a generalized linear model (Negative Binomial). Briefly, we used gene expression (the expressed genes with the average count $>$ 1) as the dependent variable and smoking status as the independent variable while accounting for confounders including age, cancer stage and histology. and

In detail, the gene expression matrix $\boldsymbol{Y}$ with N gene $\times$ P cells,

$$\boldsymbol{Y}_i = \left[y_j\right]_i$$

For a given gene $i \in \{1, 2, \cdots, N\}$ across cells $j \in \{1, 2, \cdots, P\}$, $y_{i,j}$ are assumed to follow negative binomial distribution.

$$y_{i,j} \sim NB\left(\mu_{i,j}, \phi_{i\cdot}\right)$$

$$\log\left(\mu_{i,j}\right) = \eta_{i,j}$$

$$\eta_{i,j} = \sum_{k=1}^{m} \beta_k x_{jk} = \boldsymbol{\beta} \boldsymbol{x}_j^T$$

where $NB(\mu_{i,j}, \phi_{i\cdot})$ denotes a negative binomial generalized additive model (NB-GAM) with gene-specific dispersion parameters ϕ_i. and $\mu_{i,j}$ denotes cell and gene-specific means. In addition, $\boldsymbol{\beta} = \{\beta_1, \beta_2, \cdots, \beta_m\}^T$, which are m-dimensional unknown regression parameters; $\boldsymbol{x}_j^T = \{x_{j1}, x_{j1}, \cdots, x_{jm}\}$, which are covariates including smoking status, age, cancer stage and histology for all the expressed genes with the average count $>$ 1. The model is stratified by sex and tissue. Furthermore, P values were adjusted following Benjamini & Hochberg protocol. We define a SIDEG when the absolute coefficient $|\beta| > 1$, Q-value < 0.01.

Impute cell fractions with CIBERSORTx

We first prepared and uploaded the single-cell reference sample file from GSE99254 scRNA-seq sequencing data to build a signature matrix with cell type identifiers according to the CIBERSORTx tutorial(https://cibersortx.stanford.edu/) using default parameters. Then, we prepared and uploaded the mixture datasets of tumor and normal groups obtained from Cell, 2020 (https://ars.els-cdn.com/content/image/1-s2.0-S0092867420306760-mmc3.xlsx)according to the CIBERSORTx tutorial. Since scRNA data was derived from Smart-seq2, we selected "B-mode" for batch correction. Other parameters are remained default. After running "CIBERSORTx", we inferred the cell fractions of T cell clusters in each sample with P-value measuring the confidence of the results for the deconvolution from the bulk RNA-seq. Samples with $P <$ 0.05 were included for a further study.

Markers identification and cell type annotation

We used the marker genes identified in Guo et al's study to identify Tregs and other type of T cells. The marker gene list was publicly

available and was appended to Supplementary Table 3.

ADAM12^{+} CTLA4^{+}Tregs was separated from CTLA4^{+} CD4^{+} Tregs based on the bimodal expression distribution of ADAM12. We listed the marker genes for ADAM12^{+} CTLA4^{+} Tregs that we identified in our study in supplementary Table 7. We then identified 46 DEGs between ADAM12-positive (log(scaled-expression) > -3) and negative (log (scaled-expression) < -3) populations of CTLA4^{+} CD4^{+} Tregs (See supplementary Table 8).

Then we annotated T cells using SingleR [39] based on T cell annotations of GSE99254 dataset. First, we generated a predictive model by randomly sampling 75% cells from 9055 T cells with known labels, and chose marker genes of each cell cluster as reference set to train the SingleR classifiers using the "trainSingleR" function. Then, we used "classifySingleR" to predict cell types from a query data set. The top 50 most significant differential expression genes were identified using "pairwiseTTests". "getTopMarkers" function is used to define marker genes. As a result, a total of 1013 genes were selected as marker genes for 17 clusters. The rest of 25% cells were used as a validation set. The model accuracy is 75.49%. Then we used the trained model to annotate the cell types in GSE131907 dataset and annotated total 42,106 cells into 17 cell clusters (Supplementary Table 4). The expression values were the normalized counts.

Development trajectory reconstruction by monocle

Monocle (2.18.0) was used to reconstruct the pseudotime trajectory to demonstrate the developmental process of different cell types. "differentialGeneTest" was performed to extract the signature genes and distinguish different cell types in all CD4 T cells and ADAM12$^{+/-}$ cells in CTLA4^{+} Tregs. The top 2000 significant genes were selected as the ordering genes for downstream analysis. Using "reduceDimension" and "orderCells" functions, we reconstructed the trajectories of all CD4^{+} T cells and ADAM12$^{+/-}$CTLA4^{+} Tregs and pseudotime for each cell.

Cell-Cell interaction analysis by CSOmap

To illustrate the cell-cell interaction potential of cells we used CSOmap [40] to construct a 3D pseudo space and calculate the significant interaction among T cell types. To investigate the interaction potentials of the cell types, we used two indexes, connection maps and normalized connections. We also plot the 3D interaction space to visualize the location of the cells. If two cell types are located close with each other in the 3D space, which indicates that they are more likely to interact with each other. To further investigate the interaction between different cell types. For a cluster pair, normalized connection was calculated as dividing its corresponding connection value by the product of their respective cell numbers. Normalized connections were then multiplied by 10,000. Meanwhile, to highlight the key ligand-receptor pairs function in the interaction, we also examine the contribution output by CSOmap.

Survival analysis

The TCGA LUAD data were used to evaluate the prognostic effect of individual genes or gene sets derived from specific cell clusters. The gene expression data and the clinical data were downloaded from UCSC Xena (http://xena.ucsc.edu/). Then, we used expression levels of (FOXP3 + CTLA4 + ADAM12) / (CD3D + CD3E + CD3G), to estimate the relative content of ADAM12^{+} CTLA4^{+} Tregs. As a control, we also estimated the relative content of CTLA4^{+} Tregs as a background using the formula (FOXP3 + CTLA4) / (CD3D + CD3E + CD3G). Patient cohorts were stratified into high and low expression groups by the median value of the normalized average expression of selected genes.

Results

Smoking induces gene expression aberration of t cells in peripheral blood, normal lung and tumors

We used single-cell RNA seq [22,23] and bulk-RNA seq data [35] of total 109 treatment-naïve NSCLC patients with smoking history to analyze the effect of smoking on primary tumor, distant metastases, adjacent normal tissues and peripheral blood (Fig. 1a, Supplementary Tables 1 and 2). We adopted the T cell annotation (16 T cell types) and performed a generalized linear regression using the T cell expression data from Guo et al. [22] to study the smoking-induced differentially expressed genes (SIDEGs) in blood, normal and tumor tissues in both sexes while adjusted the confounding factors including age and histology and stage (See methods). As results, we found that the effects of smoking on T cells in male and female patients are different. In normal tissues and blood, the common DEGs ($|\beta| > 1$, Q-value < 0.01) between male and female patients only accounted for 1.2% and 1.9% of all SIDEGs (Supplementary Fig. 1a and Supplementary Table 5). The common SIDEGs of T cells in tumor tissue between both sexes was higher than those in normal and blood, accounted for 7.6% (Supplementary Fig. 1a and Supplementary Table 5).

We further looked at the tissue specific smoking effects in both genders. We found that in male patients, up-SIDEGs are mainly genes related to DNA binding and repair (HIST2H2AC, HIST1H4C, TCFL5) (Fig. 1b). The number of tumor-specific SIDEGs in male ($N = 106$, 57.3%) are much higher than those in females ($N = 28$, 6.5%). And we see the Type I interferon response in multiple T cell types from tumor tissue of male patients (Fig. 1b).

On the other hand, in female patients, the most up-SIDEGs are also the common DEGs ($N = 25$) in multiple T cell types across normal, blood and tumor tissues, which are mostly interferon-induced genes and some antiapoptotic and ATP metabolic process genes (Supplementary Fig.1b). Since the number of smoking female patients is limited, we also include another single-cell RNA seq data which study the smoking's effect on the lymphocyte in peripheral blood of normal people [34], the results of which are similar with the SIDEGs in the female blood in our study (Supplementary Table 6).

These results suggest that smoking causes systemic immune response and tumor-site specific immune response in both genders with different effects.

Finally, we looked at cell-type-specific gene expression change induced by smoking. We adopted the T cell annotation (16 T cell types) from Guo et al's [22] for our study. Briefly, CD4-C1-CCR7 represents a cluster of CD4 naïve T cells; CD4-C3-CXCL13 indicates a cluster of CD4 exhausted T cells; CD4-C3-GNLY serves to represent a cluster of CD4 effector T cells. And LAYN is a known exhausted marker, therefore a cluster of CD8 exhausted T cells is indicated by CD8-C6-LAYN. Finally, Treg cells circulating in blood are indicated by CD4-C8-FOXP3 and tumor-specific Treg cells are represented by CD4-C9-CTLA4. CTLA4 is specifically expressed by Tregs in cancer [18], and mediates the down-regulation of T cell induced immune responses [41], thereby, is usually considered as an marker of activated Tregs in cancer [22,42]. Therefore, we inherited the use of CD4-C9-CTLA4 in Guo et al's study [22] to represent tumor-specific Tregs.

Then, we looked at cell-type-specific gene expression change induced by smoking. Intriguingly, there are several genes displayed cell-type-specific expression change according to the smoking status in male patients, such as ADAM12 and FANK1 are significantly up-regulated in CD4-C9-CTLA4 cells (tumor-specific Tregs) in male patients with smoking history (Fig. 1c). This finding led us to speculate that smoking may have a specific effect on tumor-specific Tregs.

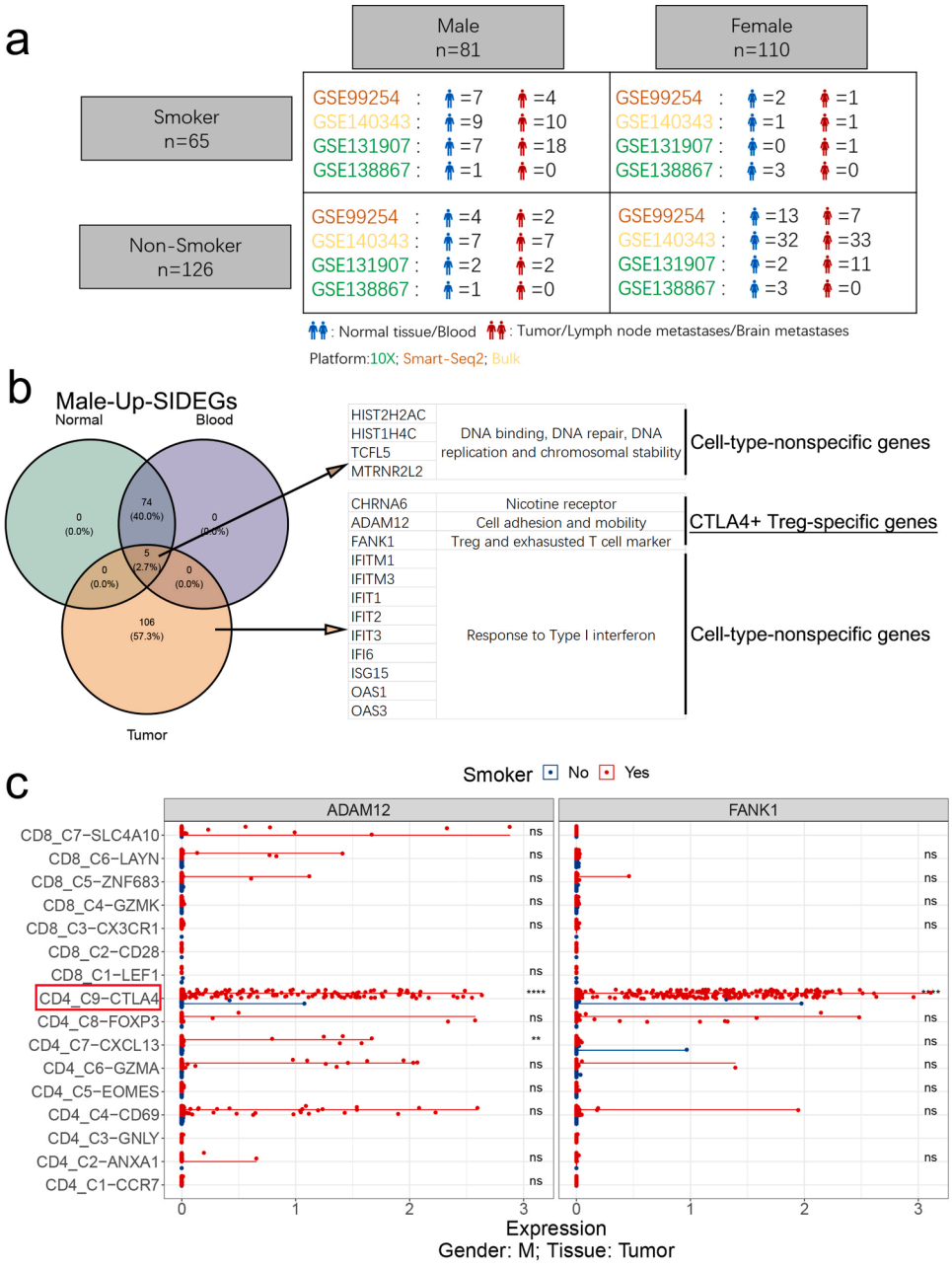

Fig. 1. Overview of datasets and analysis used in this study.(a) Description of the clinical and data information of the 109 patients, including sex, stages, treatment, tissue types, smoking history and sequencing platforms; **(b)** Venn diagram of smoking-induced up-DEGs in blood, normal and tumor sites from male patients. This plot involved 4059 cells from 6 male patients (adenocarcinoma, $n = 4$, squamous cell carcinoma, $n = 2$;Stage I, $n = 3$;Stage III, $n = 3$); **(c)** The expression levels of ADAM12 and FANK1 in 16 T cell types from the tumor sites of male patients stratified by smoking status. This plot involved 2243 cells from 6 male patients (adenocarcinoma, $n = 4$, squamous cell carcinoma, $n = 2$;Stage I, $n = 3$;Stage III, $n = 3$). *, $P < 0.05$; **, $P < 0.01$; ***, $P < 0.001$; ****, $P < 0.0001$.

Smoking induced a subset of Tregs (ADAM12$^+$ CTLA4$^+$ Tregs) in tumor microenvironment

Since we see a significant up-regulation of ADAM12 expression in tumor-enriched CTLA4$^+$ Tregs (CD4-C9-CTLA4) in male patients with smoking history, we hypothesize that smoking can induce a tumor-specific Treg subset with ADAM12 as one of the marker genes. ADAM12 is a disintegrin and metalloprotease and plays an important role in cell-cell adhesion as a sub unit of the complex with syndecans and integrins [43]. It was reported that ADAM12 is specifically expressed in both Tregs and Th17 cells in vitro, and can regulate the differentiation of Th17 cells [44]. But there are no studies to clarify the character of ADAM12$^+$ Treg neither from bulk-RNA seq analysis nor at single-cell level analysis in tumor samples. We first looked at the expression distribution of ADAM12. Indeed, ADAM12 exhibits a striking bimodal expression distribution within CD4-C9-CTLA4 cells (Fig. 2a). This indicates that we can classify CTLA4$^+$ Tregs into two subgroups: ADAM12$^-$ CTLA4$^+$ Tregs and ADAM12$^+$ CTLA4$^+$Tregs according to the expression level of ADAM12. We first obtained the top 100 marker genes of ADAM12$^+$ CTLA4$^+$ Tregs by comparing the gene expression profile of this subset of Tregs with all other T cell types ($Q < 0.01$, $\log_2$(fold change) ≥ 0.1, Supplementary Table 7). To further characterize the feature of ADAM12$^+$ CTLA4$^+$ Tregs, we compared ADAM12$^+$ CTLA4$^+$ Tregs with ADAM12$^-$ CTLA4$^+$ Tregs, and obtained a set of 46 DEGs which further defined the unique character of ADAM12$^+$ CTLA4$^+$ Tregs (Supplementary Table 8) including genes enriched in pathways like leukocyte adhesion and migration, such as ADAM12, SDC4, GCNT1, PIKFYVE, SLC16A1, IL1R1, CD177 and lipid metabolic process such as ACSL1, ACSL4, HACD1, LPIN1, SPTLC2, SACM1L, BDH2 (Fig. 2b and c). These results indicate the aberrantly active lipid metabolic process and tumor tissue-resident characteristics in ADAM12$^+$ CTLA4$^+$Tregs. In addition, we also looked at another marker gene FANK1 expression pattern, and in deed, FANK1 displays similar expression pattern as ADAM12. For example, FANK1 also shows bimodal expression

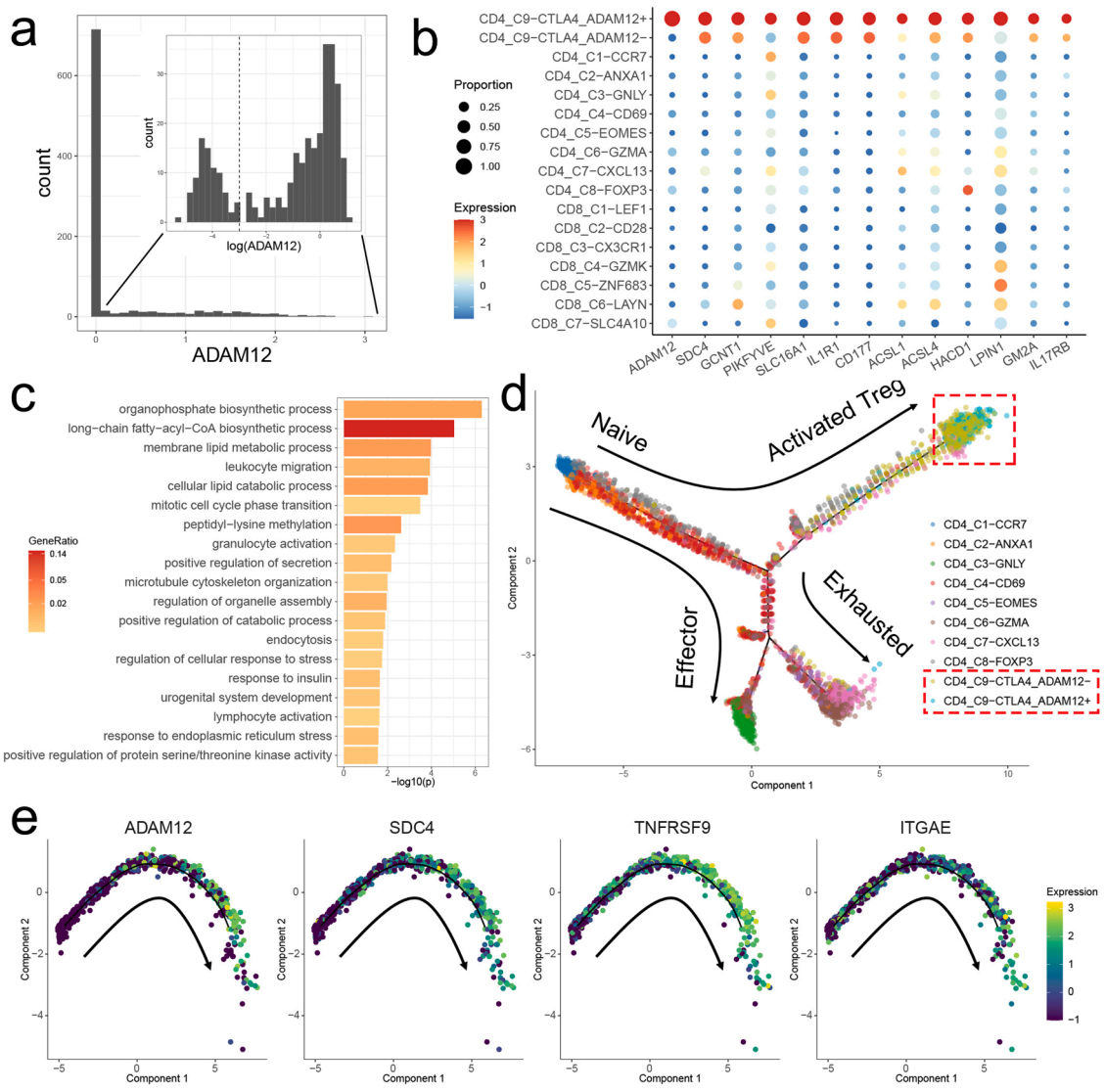

Fig. 2. Characterization of ADAM12^{+} CTLA4^{+} Tregs. **(a)** The histogram of the expression distribution of ADAM12 in CTLA4^{+} Tregs. 225 cells from 9 patients (adenocarcinoma, $n = 11$; squamous cell carcinoma, $n = 3$;Stage I, $n = 9$;Stage III, $n = 4$;Stage IV, $n = 1$) with adenocarcinoma (110 cells) and 3 patients with squamous cell carcinoma (115 cells) were identified as ADAM12^{+} CTLA4^{+} Tregs from 9055 T cells. **(b)** The expression distribution of the representative marker genes of ADAM12^{+} CTLA4^{+} Tregs in 17 T cell clusters. **(c)** GO-BP pathway enrichment analysis of 46 DEGs of ADAM12^{+} CTLA4^{+} Tregs. **(d)** The branched trajectory of CD4^{+} T cell state transition in a two-dimensional state-space inferred by Monocle 2. Each dot corresponds to one single cell, and is colored according to the cell types. Arrows indicate the transition directions.939 CTLA4^{+} Tregs from all 14 patients were involved in the pseudo time analysis. (e) CTLA4^{+} Tregs differentiation direction inferred by Monocle 2. The expression levels of ADAM12, TNFRSF9, SDC4 and ITGAE are shown along inferred trajectories.

distribution in CTLA4+ Tregs just like ADAM12 in Fig. 2a (Supplementary Fig.2) And the expression pattern of FANK1 in trajectory analysis of CTLA4^{+} Tregs is also similar as the expression levels of ADAM12. (Supplementary Fig.2)

To demonstrate the origin of ADAM12^{+} CTLA4^{+} Tregs, we used Monocle [45–47] to reconstruct the pseudo time trajectory of CD4^{+} T cells (Fig. 2d). CD4^{+} T cells displayed clear developmental trajectory from naïve CD4^{+} T cells (CD4-C1-CCR7) to three endpoints: exhausted CD4^{+}T cells (CD4-C3-CXCL13), effector CD4^{+}T cells (CD4-C3-GNLY) and activated regulatory T cells (CD4-C9-CTLA4) (Fig. 2d). More importantly, we can see that ADAM12^{+} CTLA4^{+} Tregs (CD4-C9-CTLA4-ADAM12^{+}) are located at branch endpoint and further away from the naïve CD4^{+} T cells than CD4-C8-FOXP3 (circulating Tregs) and ADAM12^{-} CTLA4^{+} Tregs (CD4-C9-CTLA4-ADAM12^{-}) (Fig. 2d), indicating that ADAM12^{+} CTLA4^{+} Tregs are at the end of CD4^{+} T cells differentiation and derived from ADAM12^{-} CTLA4^{+} Tregs. To further characterize the tumor-specific ADAM12^{+} CTLA4^{+} Tregs, we reconstructed the developmental trajectory of CTLA4^{+} Tregs (CD4-C9-CTLA4) alone. We noticed that the expression level of ADAM12 increased gradually with the development of pseudo time. TNFRSF9 is a well-defined activation marker on Tregs, highly associated with their suppressive functions. We chose TNFRSF9 as an activation indicator to reflect the level of the suppressive functions of Tregs [48,49] and we found that TNFRSF9 exhibits the similar co-expression pattern along the pseudo time trajectory as ADAM12 (Fig. 2e) suggesting ADAM12^{+} CTLA4^{+} Tregs as the endpoint of the evolution of the pseudo time trajectory and its enhanced immunosuppressive activity. Moreover, SDC4 and ITGAE were reported as the interactors of ADAM12 on cell membrane. ADAM12 can form a complex with SDC4 or ITGAE to regulate cell migration and adhesion [43]. We also observed the co- expression pattern of SDC4 (ADAM12 binding partner) and ITGAE (immune cell tissue resident marker) in pseudo time trajectory, i.e. increased expression levels along the trajectory (Fig. 2e). ADAM12, SDC4 and ITGAE can form a complex to fix cells in the extra cellular matrix (ECM)

[50], which suggest a possible mechanism underlying the tumor-resident characteristic of ADAM12$^+$ CTLA4$^+$ Tregs. Taken together, smoking-induced ADAM12$^+$ CTLA4$^+$ Tregs are activated Tregs which displayed tumor tissue resident and abnormal lipid metabolism features.

Validation of the correlation between smoking and ADAM12$^+$ CTLA4$^+$ Tregs and exploration of its biological functions

To further verify the clinical relevance and investigate possible biological functions of the tumor-specific ADAM12$^+$ CTLA4$^+$ Tregs, we used the bulk RNA sequencing dataset of a larger patient population [35], which contains 51 treatment naïve NSCLC patients. We first inferred the fraction of 17 T cell clusters in these 51 patients using the expression data of bulk-RNA seq by CIBERSORTx based on the single cell type annotation of Guo et al.'s cell type annotation [22].We first compared the fraction of ADAM12$^+$ CTLA4$^+$ Tregs between smokers and non-smokers and found that the fraction of ADAM12$^+$ CTLA4$^+$ Tregs (CD4-C9-CTLA4-ADAM12$^+$) is significantly increased in smokers both in all patients ($P = 0.010$, Wilcoxon test) and in male patients ($P = 0.040$, Wilcoxon test) (Fig. 3a, Supplementary Fig.3). Again, the number of female smokers is too small ($N = 1$) to obtain significant results but the similar trend is observed. On the other hand, ADAM12$^-$CTLA4$^+$ Tregs (CD4-C9-CTLA4-ADAM12$^-$) did not show such trend or even displayed an opposite pattern between smokers and non-smokers (Fig. 3a). These results further validated our hypothesis that smoking induces a specific subset of ADAM12$^+$ CTLA4$^+$ Tregs in tumor sites. Interestingly, we observed that the fractions of CD8-C6-LAYN (exhausted CD8$^+$ T cells)

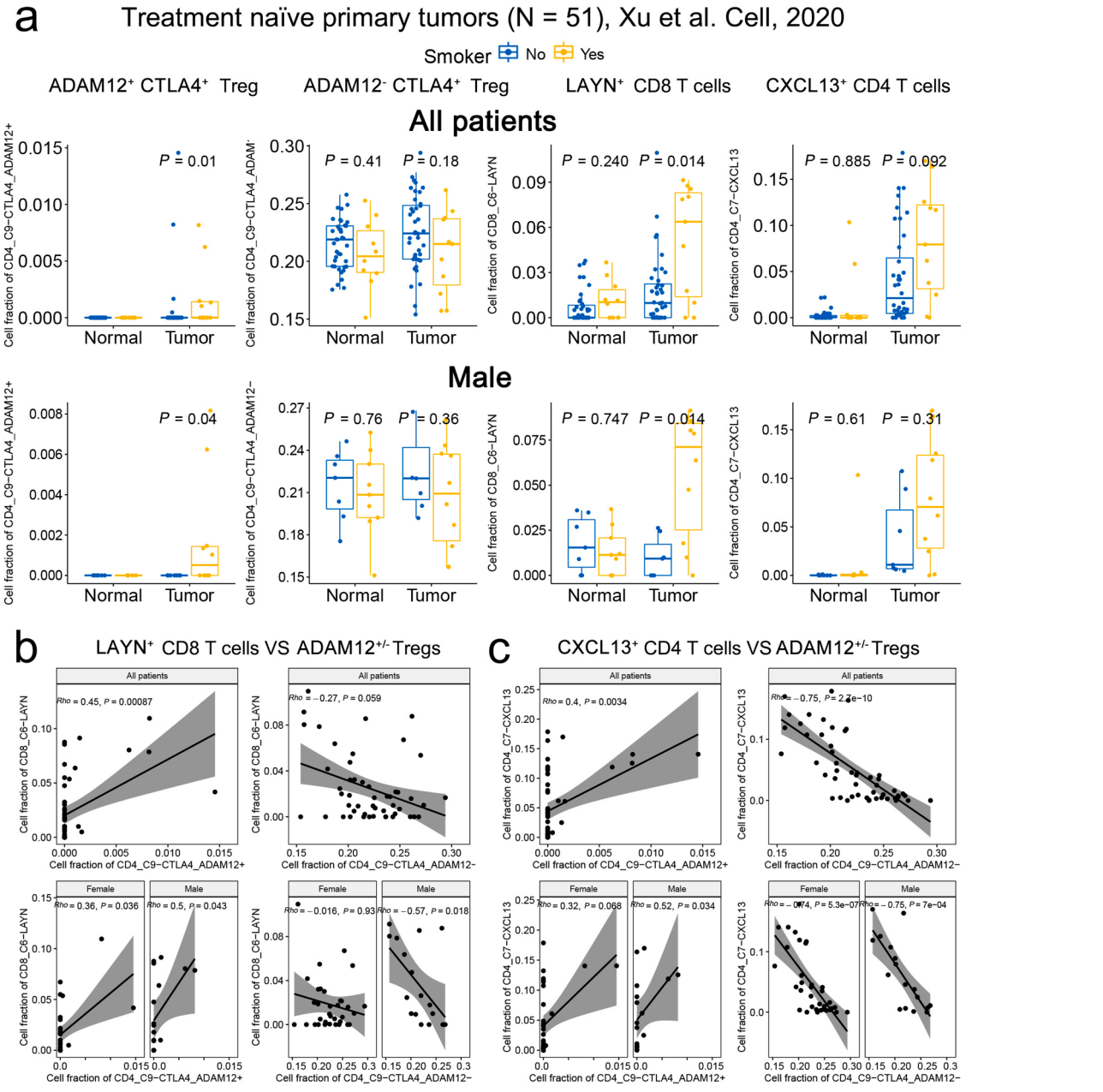

Fig. 3. The relation between smoking status and the fractions of different T cell types and the correlations among T cell types in tumor microenvironment. **(a)** The difference in the fractions of ADAM12$^+$ CTLA4$^+$ Tregs, ADAM12$^-$CTLA4$^+$Tregs, LAYN$^+$CD8$^+$ T cells and CXCL13$^+$CD4$^+$ T cells in the primary tumor sites between smokers (All patients: 11 tumor sample, 10 normal samples; Male patients: 10 tumor sample, 9 normal samples) and non-smokers (All patients: 40 tumor samples, 39 normal samples; Male patients: 7 tumor sample, 7 normal samples.). **(b)** The correlations between LAYN$^+$CD8$^+$ T cells and ADAM12$^{+/-}$CTLA4$^+$Tregs (Spearman correlation). **(c)** The correlations between CXCL13$^+$CD4 T cells and ADAM12$^{+/-}$CTLA4$^+$Tregs (Spearman correlation).

and CD4-C7-CXCL13 (exhausted CD4$^+$ T cells) are significantly or borderline significantly increased in the tumor sites in smokers (P = 0.014 and P = 0.092, Wilcoxon test) (Fig. 3a). For male patients, the fractions of CD8-C6-LAYN cells are significantly increased in smokers (P = 0.014, Wilcoxon test) while the fraction of CD4-C7-CXCL13 cells are not significant but show similar trend (P = 0.310, Wilcoxon test) (Fig. 3a). The number of female patients with smoking history is too small (N = 1). Therefore, we cannot obtain significant results in female patients (Supplementary Fig.3). These results suggest that ADAM12$^+$ CTLA4$^+$ Tregs may function through interreacting with two sets of exhausted T cell clusters, CD8-C6-LAYN or CD4-C7-CXCL13 clusters.

Therefore, we next sought to investigate the fraction correlations among clusters regardless of smoking status since the cell fractions are the outcome of smoking status. As expected, the fraction of ADAM12$^+$ CTLA4$^+$ Tregs are significantly positively correlated with the fraction of CD8-C6-LAYN (Fig. 3b) in all patients (rho = 0.45, P = 0.00087, Spearmen correlation), male patients (rho = 0.50, P = 0.043) and female patients (rho = 0.36, P = 0.036). On the contrary, ADAM12$^-$CTLA4^{+-} Tregs displayed no such correlation, or even opposite correlations with CD8-C6-LAYN in the tumor sites of all patients (rho = −0.27, P = 0.059), male patients (rho = −0.57, P = 0.018) and female patients (rho = -0.015, P = 0.93) (Fig. 3b). Similarly, the fraction of ADAM12$^+$ CTLA4$^+$ Tregs are also positively correlated with the fraction of CD4-C7-CXCL13 in all patients (rho = 0.40, P = 0.0034, Spearmen correlation), male patients (rho = 0.52, P = 0.034) and female patients (rho = 0.32, P = 0.068) (Fig. 3c). On the contrary, ADAM12$^-$CTLA4$^+$ Tregs displayed opposite correlations with CD4-C7-CXCL13 in the tumor microenvironment of all patients (rho =−0.75, $P = 2.7 \times 10^{-10}$), male patients (rho = −0.75, $P = 7.0 \times 10^{-4}$) and female patients (rho = −0.74, $P = 5.3 \times 10^{-7}$) (Fig. 3c). These results suggest that ADAM12$^+$ CTLA4$^+$ Tregs but not ADAM12$^-$CTLA4$^+$ Tregs promote more effector T cells into exhausted T cells.

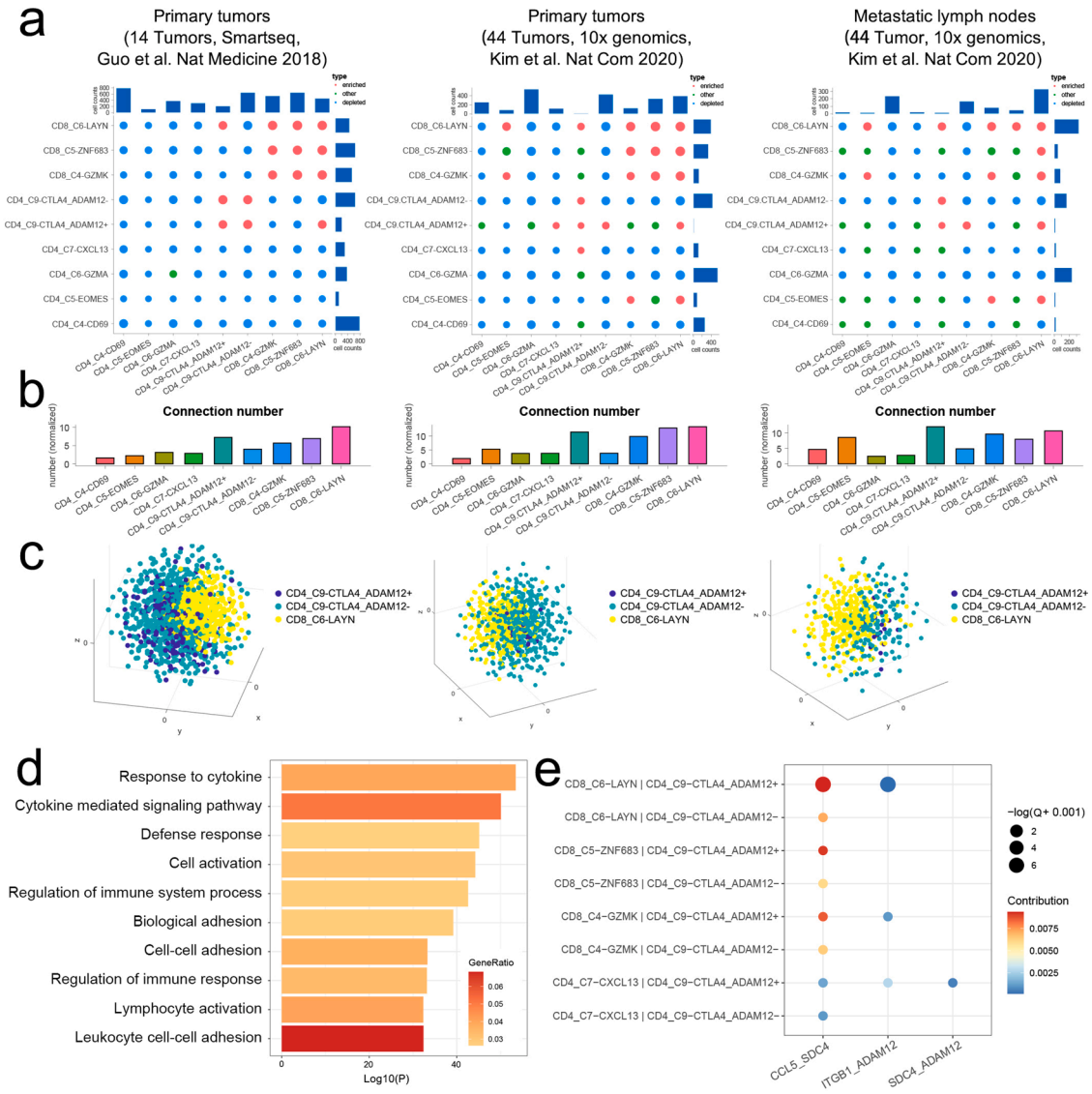

Fig. 4. Spatial reconstruction of the cell-cell communication maps of T cells in the tumor microenvironment. (a) Cell-cell communication maps of different T cells in primary tumor sites(4143 cells from Guo et al's study and 2345 cells from Kim et al's study) and metastatic lymph nodes(962 cells from Kim et al's study) from different studies. The size of the dot represents the number of communications, red dot represents the significant enrichment of intercellular communication, blue dot represents the significant depletion, and green dot represents other, ie, neither enriched or depleted (Permutation Test). **(b)** Normalized cell-cell connection number of each tumor-enriched cell cluster in primary tumor sites and metastatic lymph nodes. **(c)** CSOmap reconstruction of the spatial distance of CD8-C6-LAYN and ADAM12$^{+/-}$CTLA4$^+$Tregs in primary tumor sites and metastatic lymph nodes. **(d)** GO-BP pathway enrichment analysis of all significant ligand-receptor pairs between CD8-C6-LAYN and ADAM12$^+$ CTLA4$^+$ Tregs. **(e)** Comparison of the contribution of gene paired related to cell-cell adhesion among different cell pairs.

Single cell space reconstruction of T cell interaction network in tumor microenvironment by CSOmap

In order to further investigate the mechanism underlying these correlations, we performed CSOmap to reconstruct the 3-dimensional pseudo-space via ligand-receptor-mediated cell-cell interactions using single-cell RNA sequencing data [40]. Consistent with the correlation analysis, ADAM12^{+}CTLA4^{+} Tregs showed significant interactions with CD8-C6-LAYN by random permutation-based statistical testing in treatment naïve primary tumor and metastatic lymph nodes from both Guo *et al*'s and Kim *et al*'s studies (Fig. 4a). ADAM12^{+}CTLA4^{+} Tregs showed significant interactions with CXCL13^{+}CD4^{+} T cells in treatment naïve primary tumor from Kim *et al*'s studies (Fig. 4a). Moreover, ADAM12^{+}CTLA4^{+} Tregs have more normalized connections than ADAM12^{-}CTLA4^{+}Tregs suggesting ADAM12^{+}CTLA4^{+} Tregs are more actively communicate with other cell types than ADAM12^{-}CTLA4^{+} Tregs (Fig. 4b). Importantly, ADAM12^{+}CTLA4^{+} Tregs locate physically closer to CD8-C6-LAYN than ADAM12^{-}CTLA4^{+} Tregs in both primary tumor sites and metastatic lymph nodes according to the 3D-space reconstruction (Fig. 4c). Similarly, ADAM12^{+} CTLA4^{+} Tregs also locate closer to CD4-C7-CXCL13 than ADAM12^{-}CTLA4^{+}Tregs in the primary tumor sites from both Guo's and Kim's studies but not in metastatic lymph nodes (Supplementary Fig. 4), which may probably due to the less connections of CD4-C7-CXCL13 than CD8-C6-LAYN (Fig. 4b) or the limited number of CD4-C7-CXCL13 detected in metastatic lymph nodes. (Supplementary Fig.4) In addition, we also looked at the cell-cell interaction maps in male and female patients, respectively. As a result, the significant interaction between ADAM12^{+}CTLA4^{+} Tregs and CD8-C6-LAYN is conserved in both genders (Supplementary Fig.5).

By analyzing the dominant ligand-receptor pairs contributing to this spatial organization, we identified 119 significant ligand-receptor pairs that contribute to the interaction between ADAM12^{+}CTLA4^{+} Tregs and CD8-C6-LAYN (Supplementary Fig.6). These interaction pairs include KLRD1-HLA-B, CD8A-LCK, KLRD1-HLA-E, CCL5-CXCR3, CCL5-SDC4, ADAM12-ITGB1 pairs, and are enriched in pathways such as regulation of immune response and cell-cell adhesion (Fig. 4d). We further analyzed the cell-cell adhesion pairs and found that the CCL5-SDC4 and ITGB1-ADAM12 ligand-receptor interactions contribute most in CD8-C6-LAYN and ADAM12^{+}CTLA4^{+} Tregs pairs, compared with other cell pairs (Fig. 4e), further supporting the hypothesis that ADAM12^{+}CTLA4^{+} Tregs induce exhaustion of effector T cells through cell-cell adhesion by ADAM12-ITGB1 and SDC4-CCL5 interaction.

ADAM12^{+} CTLA4^{+} Tregs predicts overall survival of NSCLC patients

Tregs promote tumor progression by direct inhibition of antitumor effector CD4^{+} and CD8^{+} T cells and are correlated with a poor prognosis [51]. In order to investigate if ADAM12^{+}CTLA4^{+} Tregs are more pro-tumor than ADAM12^{-}CTLA4^{+} Tregs, we took advantage of the survival information from lung adenocarcinoma (LUAD) dataset from TCGA to evaluate the prognostic value of ADAM12^{+}CTLA4^{+} Tregs. We first estimated the relative content of ADAM12^{+}CTLA4^{+} Tregs or CTLA4^{+} Tregs by the median value of the normalized average expression of selected genes (See Methods). Patient cohorts were grouped into high and low expression groups. As a result, patient group with expression of ADAM12^{+} CTLA4^{+} FOXP3^{+}signature genes showed significantly worse overall survival (P = 0.014, Log-Rank test, Fig. 5a). As a background comparison, patient group with expression of CTLA4^{+} FOXP3^{+}signature genes showed worse but not significant overall survival (P = 0.06, Log-Rank test, Fig. 5b). These results suggest that compared to traditional tumor-infiltration Tregs (CTLA4^{+} FOXP3^{+}), ADAM12^{+}CTLA4^{+} Tregs showed increased predictive power and deserve further investigation for clinical applications. Of note, the treatment information such as chemotherapy, radiation therapy or immunotherapy is largely unknown for the TCGA cohort. The survival outcome is the integrated outcome from all those treatments. Hence, although the treatment varies among patients, the predicative power of ADAM12^{+}CTLA4^{+} Tregs is consistent.

Discussion

The relationship between smoking and immune systems has been investigated extensively [52,53].Cigarette smoke has both pro-inflammatory and immune-suppressive effects on the immune system [54]. However, it is not clear if smoking can impact the TIME in the settings of lung cancer at a single cell resolution.

In this study, we integrated single-cell RNA-seq and bulk RNA-seq data from several studies to investigate smoking's impact on treatment naïve non-small cell lung cancer patients and found that smoking induced ADAM12 upregulation in tumor-specific Treg cells. These ADAM12^{+}Tregs highly express Treg active marker TNFRSF9, and actively interact with exhausted T cells.

One limitation in our study is the limited number of female patients. Although we observed ISGs up-regulation in multiple T cell types across blood, normal tissue and tumor tissue of one female smoker patient, we cannot draw any conclusive results from only one female patient. On the other hand, we observed Type I interferon responses specifically in tumor tissues of male smoker patients. We hypothesize that the differences that we observed from male and female patients are probably due to two reasons. First, smoking can induce both acute effects and chronic effects on the immune system and has both pro-inflammatory and immunosuppressive effects [54]. Therefore, the systematic Type I interferon responses in this one female patient are probably due to the acute effects of smoking. Second, sex difference contributes to the immune responses against infection and antitumor immunity [55]. Women have an enhance immune reactivity compared to men which makes

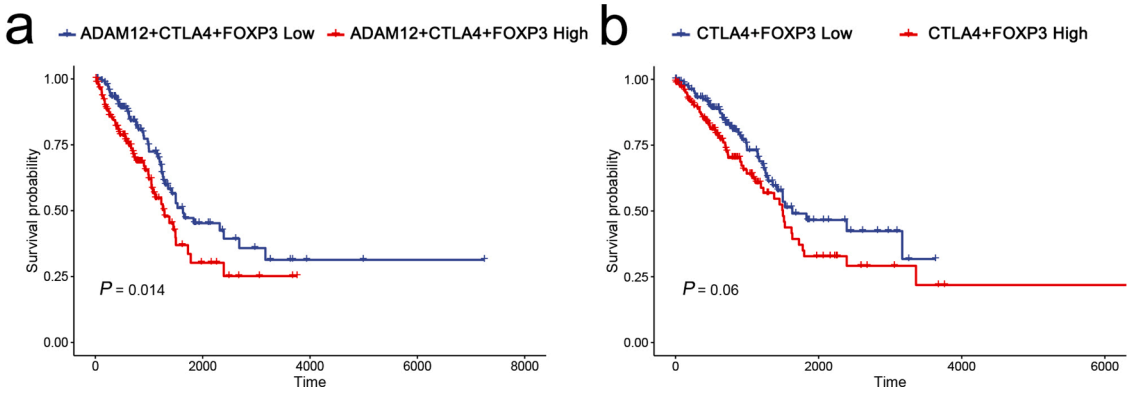

Fig. 5. Survival Analysis of TCGA LUAD patients (n = 288, male=164, female =124) with different expression levels of Treg signature genes. **(a)** The Kaplan–Meier overall survival curves of TCGA LUAD patients grouped by the gene signature of ADAM12^{+} CTLA4^{+} Tregs. P value was calculated by log-rank test. **(b)** The Kaplan–Meier overall survival curves of TCGA LUAD patients grouped by the gene signature of CTLA4^{+} Tregs. P value was calculated by log-rank test.

them have higher immune responses to smoking than men do [56]. However, due to the limited number of female smoker patients, we cannot draw confident conclusions from our analysis of female patients. In order to obtain any conclusive results, we have to include more female smoker patients in the further study.

Another limitation in our study is that the term of "Smoker" in our study is defined according to the published studies and no detailed smoking history is available. Therefore, we cannot further characterize the effect of smoking history on gene expression changes in different immune cell types. It has been recognized that smoking-induced genomic and epigenomic aberrations are related to the smoking dose and duration [8]. However, in this current study, we are unable to analyze the dose and duration effect of smoking on the tumor microenvironment.

Through ligand-receptor analysis, we deduce that ADAM12-Syndecan-Integrin complex between ADAM12$^+$ CTLA4$^+$ Tregs and LAYN$^+$ CD8 T cells is probably the cause of their physical interaction. Thus, our hypothesis is that smoking induced CTLA4$^+$ Tregs tumor tissue residency and interacting more actively with exhausted T cells. This is an important clue for immune checkpoint blockade therapy in lung cancer patient with smoking history. It has been recognized that smokers with non-small cell lung cancer (NSCLC) respond better to the inhibition of programmed cell death-1 (PD-1) with pembrolizumab than non-smokers do [6]. Liu et al. showed that smoking impact the prognostic value of circulating Tregs in advance NSCLC patients [57]. However, the mechanism is not clear. In our study, we suggested a possible mechanism that smoking induced a tumor-resident and more activated Tregs with aberrant lipid metabolism which leads to increased inhibition of effector cells and increased load of exhausted T cells. Therefore, in patients with smoking history, more exhausted T cells can be reinvigorated to effector T cells by PD-1 blockade. In turn, these smoking patients showed better response rate of immune checkpoint blockade therapy.

Conclusion

We found smoking induced specific expression of ADAM12 in tumor-specific Tregs in treatment naïve NSCLC patients. These ADAM12$^+$ Tregs highly express Treg active marker TNFRSF9 and have enhanced activity in lipid metabolism and cell adhesion pathways. ADAM12$^+$ Tregs also show an abnormal interaction activity with exhausted T cells compared with ADAM12$^-$Tregs.In addition, patients with signature of ADAM12$^+$ Tregs is associated with poor prognosis in TCGA LUAD cohort. Our findings demonstrated that smoking impact the tumor microenvironment induced a subset of Tregs with enhanced immunosuppression activity. Our findings suggested possible mechanism underlying the heterogeneity of NSCLC patients. Moreover, we provide a potential biomarker and therapeutic target, ADAM12, for precision immunotherapy of lung cancer patients with smoking history.

Author contribution

The project was conceived and directed by Ying Zhou and Qiyuan Li. Data analysis was performed by Yudi Hu and Chaoqun Xu, with assistance from Yuanyuan Zeng, Fengyang Cao and Hongkun Fang. Single cell annotation was carried out by Chaoqun Xu, Xu, Hongkun Fang, Jintao Guoand Jun Ren. The trajectory analysis was performed by Yudi Hu. The manuscript was written by Ying Zhou, Yudi Hu and Qiyuan Li. All authors read and approved the final manuscript.

Declaration of Competing Interest

The authors declare that they have no known competing financial interests or personal relationships that could have appeared to influence the work reported in this paper.

Acknowledgments

We would like to thank Yaning Hu, Huanhuan Liu, Zhiyu You and Qinwei Chen for constructive discussions.

Funding

This research is supported by the Young Scientists Fund of the National Natural Science Foundation of China to Ying Zhou [Grant no. 81802823] and the Fundamental Research Funds for the Chinese Central Universities to Qiyuan Li [Grant no.20720190101].

Supplementary materials

Supplementary material associated with this article can be found, in the online version, at doi:10.1016/j.tranon.2021.101261.

References

[1] R.S. Herbst, J.V. Heymach, S.M. Lippman, Lung Cancer, N. Engl. J. Med. 359 (2008) 1367–1380, https://doi.org/10.1056/NEJMra0802714, https://doi.org/.
[2] S.J. Lee, J. Lee, Y.S. Park, C.-.H. Lee, S.-.M. Lee, J.-.J. Yim, et al., Impact of smoking on mortality of patients with non-small cell lung cancer, Thorac Cancer 5 (2014) 43–49, https://doi.org/10.1111/1759-7714.12051, https://doi.org/.
[3] L-M Lu, C.C.J. Zavitz, B. Chen, S. Kianpour, Y. Wan, M.R. Stämpfli, Cigarette smoke impairs NK cell-dependent tumor immune surveillance, J. Immunol. 178 (2007) 936–943, https://doi.org/10.4049/jimmunol.178.2.936, https://doi.org/.
[4] S.P. Ng, A.E. Silverstone, Z.-.W. Lai, J.T. Zelikoff, Effects of prenatal exposure to cigarette smoke on offspring tumor susceptibility and associated immune mechanisms, Toxicol. Sci. 89 (2006) 135–144, https://doi.org/10.1093/toxsci/kfj006, https://doi.org/.
[5] A. Karlsson, M. Ringnér, M. Lauss, J. Botling, P. Micke, M. Planck, et al., Genomic and transcriptional alterations in lung adenocarcinoma in relation to smoking history, Clin. Cancer Res. 20 (2014) 4912–4924, https://doi.org/10.1158/1078-0432.CCR-14-0246, https://doi.org/.
[6] L.B. Alexandrov, Y.S. Ju, K. Haase, P. Van Loo, I. Martincorena, S. Nik-Zainal, et al., Mutational signatures associated with tobacco smoking in human cancer, Science 354 (2016) 618–622, https://doi.org/10.1126/science.aag0299, https://doi.org/.
[7] G.P. Pfeifer, M.F. Denissenko, M. Olivier, N. Tretyakova, S.S. Hecht, P. Hainaut, Tobacco smoke carcinogens, DNA damage and p53 mutations in smoking-associated cancers, Oncogene 21 (2002) 7435–7451, https://doi.org/10.1038/sj.onc.1205803, https://doi.org/.
[8] K. Liu, J. Guo, K. Liu, P. Fan, Y. Zeng, C. Xu, et al., Integrative analysis reveals distinct subtypes with therapeutic implications in KRAS-mutant lung adenocarcinoma, EBioMedicine 36 (2018) 196–208, https://doi.org/10.1016/j.ebiom.2018.09.034, https://doi.org/.
[9] M. Yarchoan, B.A. Johnson, E.R. Lutz, D.A. Laheru, E.M. Jaffee, Targeting neoantigens to augment antitumour immunity, Nat. Rev. Cancer 17 (2017) 209–222, https://doi.org/10.1038/nrc.2016.154, https://doi.org/.
[10] N.A. Rizvi, M.D. Hellmann, A. Snyder, P. Kvistborg, V. Makarov, J.J. Havel, et al., Mutational landscape determines sensitivity to PD-1 blockade in non–small cell lung cancer, Science 348 (2015) 124–128, https://doi.org/10.1126/science.aaa1348, https://doi.org/.
[11] J. Norum, C. Nieder, Tobacco smoking and cessation and PD-L1 inhibitors in non-small cell lung cancer (NSCLC): a review of the literature, ESMO Open 3 (2018), https://doi.org/10.1136/esmoopen-2018-000406 https://doi.org/.
[12] J. Mo, X. Hu, L. Gu, B. Chen, P.A. Khadaroo, Z. Shen, et al., Smokers or non-smokers: who benefits more from immune checkpoint inhibitors in treatment of malignancies? An up-to-date meta-analysis, World J. Surg. Oncol. 18 (2020) 15, https://doi.org/10.1186/s12957-020-1792-4, https://doi.org/.
[13] A.C. Huang, M.A. Postow, R.J. Orlowski, R. Mick, B. Bengsch, S. Manne, et al., T-cell invigoration to tumour burden ratio associated with anti-PD-1 response, Nature 545 (2017) 60–65, https://doi.org/10.1038/nature22079, https://doi.org/.
[14] P.C. Tumeh, C.L. Harview, J.H. Yearley, I.P. Shintaku, E.J.M. Taylor, L. Robert, et al., PD-1 blockade induces responses by inhibiting adaptive immune resistance, Nature 515 (2014) 568–571, https://doi.org/10.1038/nature13954, https://doi.org/.
[15] Y. Ohue, H. Nishikawa, Regulatory T (Treg) cells in cancer: can Treg cells be a new therapeutic target? Cancer Sci. 110 (2019) 2080–2089, https://doi.org/10.1111/cas.14069, https://doi.org/.
[16] Y. Togashi, K. Shitara, H. Nishikawa, Regulatory T cells in cancer immunosuppression — Implications for anticancer therapy, Nat. Rev. Clin. Oncol. 16 (2019) 356–371, https://doi.org/10.1038/s41571-019-0175-7, https://doi.org/.
[17] C. Li, P. Jiang, S. Wei, X. Xu, J. Wang, Regulatory T cells in tumor microenvironment: new mechanisms, potential therapeutic strategies and future prospects, Mol. Cancer 19 (2020) 116, https://doi.org/10.1186/s12943-020-01234-1, https://doi.org/.

[18] N. Sobhani, D.R. Tardiel-Cyril, A. Davtyan, D. Generali, R. Roudi, Y. Li, CTLA-4 in regulatory T cells for cancer immunotherapy, Cancers (Basel) 13 (2021) 1440, https://doi.org/10.3390/cancers13061440, https://doi.org/.
[19] A. Oshlack, M.D. Robinson, M.D. Young, From RNA-seq reads to differential expression results, Genome Biol. 11 (2010) 220, https://doi.org/10.1186/gb-2010-11-12-220, https://doi.org/.
[20] J.-.S. Seo, Y.S. Ju, W.-.C. Lee, J.-.Y. Shin, J.K. Lee, T. Bleazard, et al., The transcriptional landscape and mutational profile of lung adenocarcinoma, Genome Res. 22 (2012) 2109–2119, https://doi.org/10.1101/gr.145144.112, https://doi.org/.
[21] S.-.S. Han, W.J. Kim, Y. Hong, S.-.H. Hong, S.-.J. Lee, D.R. Ryu, et al., RNA sequencing identifies novel markers of non-small cell lung cancer, Lung Cancer 84 (2014) 229–235, https://doi.org/10.1016/j.lungcan.2014.03.018, https://doi.org/.
[22] X. Guo, Y. Zhang, L. Zheng, C. Zheng, J. Song, Q. Zhang, et al., Global characterization of T cells in non-small-cell lung cancer by single-cell sequencing, Nat. Med. 24 (2018) 978–985, https://doi.org/10.1038/s41591-018-0045-3, https://doi.org/.
[23] N. Kim, H.K. Kim, K. Lee, Y. Hong, J.H. Cho, J.W. Choi, et al., Single-cell RNA sequencing demonstrates the molecular and cellular reprogramming of metastatic lung adenocarcinoma, Nat. Commun. 11 (2020) 2285, https://doi.org/10.1038/s41467-020-16164-1, https://doi.org/.
[24] K.-.T. Kim, H.W. Lee, H.-.O. Lee, S.C. Kim, Y.J. Seo, W. Chung, et al., Single-cell mRNA sequencing identifies subclonal heterogeneity in anti-cancer drug responses of lung adenocarcinoma cells, Genome Biol. 16 (2015) 127, https://doi.org/10.1186/s13059-015-0692-3, https://doi.org/.
[25] I. Tirosh, B. Izar, S.M. Prakadan, M.H. Wadsworth, D. Treacy, J.J. Trombetta, et al., Dissecting the multicellular ecosystem of metastatic melanoma by single-cell RNA-seq, Science 352 (2016) 189–196, https://doi.org/10.1126/science.aad0501, https://doi.org/.
[26] Y. Zhou, D. Yang, Q. Yang, X. Lv, W. Huang, Z. Zhou, et al., Single-cell RNA landscape of intratumoral heterogeneity and immunosuppressive microenvironment in advanced osteosarcoma, Nat. Commun. 11 (2020) 6322, https://doi.org/10.1038/s41467-020-20059-6, https://doi.org/.
[27] M. Binnewies, E.W. Roberts, K. Kersten, V. Chan, D.F. Fearon, M. Merad, et al., Understanding the tumor immune microenvironment (TIME) for effective therapy, Nat. Med. 24 (2018) 541–550, https://doi.org/10.1038/s41591-018-0014-x, https://doi.org/.
[28] M.R. Junttila, F.J. de Sauvage, Influence of tumour micro-environment heterogeneity on therapeutic response, Nature 501 (2013) 346–354, https://doi.org/10.1038/nature12626, https://doi.org/.
[29] Q. Wang, B. Hu, X. Hu, H. Kim, M. Squatrito, L. Scarpace, et al., Tumor evolution of glioma-intrinsic gene expression subtypes associates with immunological changes in the microenvironment, Cancer Cell 32 (2017) 42–56, https://doi.org/10.1016/j.ccell.2017.06.003, e6https://doi.org/.
[30] L. Zhang, X. Yu, L. Zheng, Y. Zhang, Y. Li, Q. Fang, et al., Lineage tracking reveals dynamic relationships of T cells in colorectal cancer, Nature 564 (2018) 268–272, https://doi.org/10.1038/s41586-018-0694-x, https://doi.org/.
[31] C. Zheng, L. Zheng, J.-.K. Yoo, H. Guo, Y. Zhang, X. Guo, et al., Landscape of infiltrating T cells in liver cancer revealed by single-cell sequencing, Cell 169 (2017) 1342–1356, https://doi.org/10.1016/j.cell.2017.05.035, e16https://doi.org/.
[32] K.C. Goldfarbmuren, N.D. Jackson, S.P. Sajuthi, N. Dyjack, K.S. Li, C.L. Rios, et al., Dissecting the cellular specificity of smoking effects and reconstructing lineages in the human airway epithelium, Nat. Commun. 11 (2020) 2485, https://doi.org/10.1038/s41467-020-16239-z, https://doi.org/.
[33] G.E. Duclos, V.H. Teixeira, P. Autissier, Y.B. Gesthalter, M.A. Reinders-Luinge, R. Terrano, et al., Characterizing smoking-induced transcriptional heterogeneity in the human bronchial epithelium at single-cell resolution, Sci. Adv. 5 (2019) eaaw3413, https://doi.org/10.1126/sciadv.aaw3413, https://doi.org/.
[34] S.N. Martos, M.R. Campbell, O.A. Lozoya, X. Wang, B.D. Bennett, I.J.B. Thompson, et al., Single-cell analyses identify dysfunctional CD16+ CD8 T Cells in smokers, Cell Rep. Med. 1 (2020), 100054, https://doi.org/10.1016/j.xcrm.2020.100054 https://doi.org/.
[35] J.-.Y. Xu, C. Zhang, X. Wang, L. Zhai, Y. Ma, Y. Mao, et al., Integrative proteomic characterization of human lung adenocarcinoma, Cell 182 (2020) 245–261, https://doi.org/10.1016/j.cell.2020.05.043, e17https://doi.org/.
[36] J. Cao, M. Spielmann, X. Qiu, X. Huang, D.M. Ibrahim, A.J. Hill, et al., The single-cell transcriptional landscape of mammalian organogenesis, Nature 566 (2019) 496, https://doi.org/10.1038/s41586-019-0969-x, https://doi.org/.
[37] C. Trapnell, D. Cacchiarelli, J. Grimsby, P. Pokharel, S. Li, M. Morse, et al., The dynamics and regulators of cell fate decisions are revealed by pseudotemporal ordering of single cells, Nat. Biotechnol. 32 (2014) 381–386, https://doi.org/10.1038/nbt.2859, https://doi.org/.
[38] X. Qiu, Q. Mao, Y. Tang, L. Wang, R. Chawla, H.A. Pliner, et al., Reversed graph embedding resolves complex single-cell trajectories, Nat. Method. 14 (2017) 979–982, https://doi.org/10.1038/nmeth.4402, https://doi.org/.
[39] D. Aran, A.P. Looney, L. Liu, E. Wu, V. Fong, A. Hsu, et al., Reference-based analysis of lung single-cell sequencing reveals a transitional profibrotic macrophage, Nat. Immunol. 20 (2019) 163–172, https://doi.org/10.1038/s41590-018-0276-y, https://doi.org/.
[40] X. Ren, G. Zhong, Q. Zhang, L. Zhang, Y. Sun, Z. Zhang, Reconstruction of cell spatial organization from single-cell RNA sequencing data based on ligand-receptor mediated self-assembly, Cell Res. 30 (2020) 763–778, https://doi.org/10.1038/s41422-020-0353-2, https://doi.org/.
[41] B. Rowshanravan, N. Halliday, D.M. Sansom, CTLA-4: a moving target in immunotherapy, Blood 131 (2018) 58–67, https://doi.org/10.1182/blood-2017-06-741033, https://doi.org/.
[42] F. Marangoni, A. Zhakyp, M. Corsini, S.N. Geels, E. Carrizosa, M. Thelen, et al., Expansion of tumor-associated Treg cells upon disruption of a CTLA-4-dependent feedback loop, Cell 184 (2021) 3998–4015, https://doi.org/10.1016/j.cell.2021.05.027, e19https://doi.org/.
[43] M. Kveiborg, R. Albrechtsen, J.R. Couchman, U.M. Wewer, Cellular roles of ADAM12 in health and disease, Int. J. Biochem. Cell Biol. 40 (2008) 1685–1702, https://doi.org/10.1016/j.biocel.2008.01.025, https://doi.org/.
[44] A.X. Zhou, A. El Hed, F. Mercer, L. Kozhaya, D. Unutmaz, The Metalloprotease ADAM12 regulates the effector function of human Th17 cells, PLoS One 8 (2013) e81146, https://doi.org/10.1371/journal.pone.0081146, https://doi.org/.
[45] X. Qiu, Q. Mao, Y. Tang, L. Wang, R. Chawla, H.A. Pliner, et al., Reversed graph embedding resolves complex single-cell trajectories, Nat. Method. 14 (2017) 979.
[46] C. Trapnell, D. Cacchiarelli, J. Grimsby, P. Pokharel, S. Li, M. Morse, et al., The dynamics and regulators of cell fate decisions are revealed by pseudotemporal ordering of single cells, Nat. Biotechnol. 32 (2014) 381.
[47] X. Qiu, A. Hill, J. Packer, D. Lin, Y.-.A. Ma, C. Trapnell, Single-cell mRNA quantification and differential analysis with Census, Nat. Method. 14 (2017) 309–315, https://doi.org/10.1038/nmeth.4150, https://doi.org/.
[48] M. Nagar, J. Jacob-Hirsch, H. Vernitsky, Y. Berkun, S. Ben-Horin, N. Amariglio, et al., TNF activates a NF-κB–regulated cellular program in human CD45RA– regulatory T cells that modulates their suppressive function, J. Immunol. 184 (2010) 3570–3581, https://doi.org/10.4049/jimmunol.0902070, https://doi.org/.
[49] P. Bacher, F. Heinrich, U. Stervbo, M. Nienen, M. Vahldieck, C. Iwert, et al., Regulatory T cell specificity directs tolerance versus allergy against aeroantigens in humans, Cell 167 (2016) 1067–1078, https://doi.org/10.1016/j.cell.2016.09.050, e16https://doi.org/.
[50] M. Kveiborg, R. Albrechtsen, J.R. Couchman, U.M. Wewer, Cellular roles of ADAM12 in health and disease, Int. J. Biochem. Cell Biol. 40 (2008) 1685–1702, https://doi.org/10.1016/j.biocel.2008.01.025, https://doi.org/.
[51] A. Facciabene, G.T. Motz, G. Coukos, T-regulatory cells: key players in tumor immune escape and angiogenesis, Cancer Res. 72 (2012) 2162–2171, https://doi.org/10.1158/0008-5472.CAN-11-3687, https://doi.org/.
[52] M. Sopori, Effects of cigarette smoke on the immune system, Nat. Rev. Immunol. 2 (2002) 372–377, https://doi.org/10.1038/nri803, https://doi.org/.
[53] P.G. Holt, D. Keast, Environmentally induced changes in immunological function: acute and chronic effects of inhalation of tobacco smoke and other atmospheric contaminants in man and experimental animals, Bacteriol. Rev. 41 (1977) 205–216.
[54] M.R. Stämpfli, G.P. Anderson, How cigarette smoke skews immune responses to promote infection, lung disease and cancer, Nat. Rev. Immunol. 9 (2009) 377–384, https://doi.org/10.1038/nri2530, https://doi.org/.
[55] B.C. Özdemir, G.-.P. Dotto, Sex hormones and anticancer immunity, Clin. Cancer Res. 25 (2019) 4603–4610, https://doi.org/10.1158/1078-0432.CCR-19-0137, https://doi.org/.
[56] M. Pierdominici, A. Maselli, T. Colasanti, A.M. Giammarioli, F. Delunardo, D. Vacirca, et al., Estrogen receptor profiles in human peripheral blood lymphocytes, Immunol. Lett. 132 (2010) 79–85, https://doi.org/10.1016/j.imlet.2010.06.003, https://doi.org/.
[57] C. Liu, Y. Sun, J. Yue, J. Yu, Prognostic interaction of smoking history with circulating regulatory T cells in advanced non-small cell lung cancer, JCO 37 (2019), https://doi.org/10.1200/JCO.2019.37.15_suppl.e14030 e14030–e14030https://doi.org/.